Molecules and Cells

Tazarotene-Induced Gene 1 Interacts with DNAJC8 and Regulates Glycolysis in Cervical Cancer Cells

Chun-Hua Wang[1,2], Rong-Yaun Shyu[3], Chang-Chieh Wu[4], Mao-Liang Chen[5], Ming-Cheng Lee[5], Yi-Yin Lin[5], Lu-Kai Wang[6], Shun-Yuan Jiang[5], and Fu-Ming Tsai[5,*]

[1]Department of Dermatology, Taipei Tzuchi Hospital, The Buddhist Tzuchi Medical Foundation, New Taipei City 231, Taiwan, [2]School of Medicine, Tzu Chi University, Hualien 970, Taiwan, [3]Department of Internal Medicine, Taipei Tzuchi Hospital, The Buddhist Tzuchi Medical Foundation, New Taipei City 231, Taiwan, [4]Department of Surgery, Tri-Service General Hospital Keelung Branch, National Defense Medical Center, Keelung 202, Taiwan, [5]Department of Research, Taipei Tzuchi Hospital, The Buddhist Tzuchi Medical Foundation, New Taipei City 231, Taiwan, [6]Radiation Biology Core Laboratory, Institute for Radiological Research, Chang Gung University/Chang Gung Memorial Hospital, Linkou, Taoyuan 333, Taiwan
*Correspondence: afu2215@gmail.com
http://dx.doi.org/10.14348/molcells.2018.2347
www.molcells.org

The tazarotene-induced gene 1 (TIG1) protein is a retinoid-inducible growth regulator and is considered a tumor suppressor. Here, we show that DnaJ heat shock protein family member C8 (DNAJC8) is a TIG1 target that regulates glycolysis. Ectopic DNAJC8 expression induced the translocation of pyruvate kinase M2 (PKM2) into the nucleus, subsequently inducing glucose transporter 1 (GLUT1) expression to promote glucose uptake. Silencing either DNAJC8 or PKM2 alleviated the upregulation of GLUT1 expression and glucose uptake induced by ectopic DNAJC8 expression. TIG1 interacted with DNAJC8 in the cytosol, and this interaction completely blocked DNAJC8-mediated PKM2 translocation and inhibited glucose uptake. Furthermore, increased glycose uptake was observed in cells in which TIG1 was silenced. In conclusion, TIG1 acts as a pivotal repressor of DNAJC8 to enhance glucose uptake by partially regulating PKM2 translocation.

Keywords: DNAJC8, glucose transporter, glycolysis, HSP40, pyruvate kinase M2, tazarotene-induced gene 1

INTRODUCTION

Unlike normal cells, cancer cells possess a distinct metabolism that prefers inefficient glucose metabolism instead of mitochondrial oxidative phosphorylation. The phenomenon is referred to as the Warburg effect (Warburg et al., 1927). Cancer cells rely on incomplete glucose metabolism, which increases glycolytic flux and glucose uptake and produces large amounts of lactate rather than synthesizing ATP (Li et al., 2016). Due to the increasing need for glycolysis, cancer cells are proficient in transporting extracellular glucose across the cell membrane into the cytoplasm by upregulating the expression of glucose transporter (GLUT) (Carvalho et al., 2011; Medina and Owen, 2002; Yu et al., 2017). To date, 14 GLUT proteins have been shown to be expressed in humans, and they are categorized into 3 classes based on sequence similarity (Mueckler and Thorens, 2013). GLUT1 is likely one of the most extensively studied proteins of all membrane transport systems. GLUT1 is generally undetectable in normal epithelial tissues, but the overexpression of GLUT1 has been reported in various cancers and was shown to lead to increased glucose uptake into the cytoplasm of tumor cells (Yu et al., 2017).

Received 11 December, 2017; revised 20 February, 2018; accepted 20 March, 2018; published online 14 June, 2018

eISSN: 0219-1032

Tazarotene-induced gene 1 (TIG1) was identified in skin graft cultures treated with the synthetic retinoid tazarotene (Nagpal et al., 1996) and has also been identified as retinoic acid receptor responder 1 (RARRES1). TIG1 is expressed at high levels in benign or well-differentiated prostate and colon tissues (Jing et al., 2002; Wu et al., 2006), but CpG hypermethylation of the TIG1 promoter leads to the downregulation of TIG1 expression in cancer tissues derived from the liver (Chen et al., 2014), prostate (Jing et al., 2002; Zhang et al., 2004), head and neck (Kwok et al., 2009; Yanatatsaneejit et al., 2008), esophagus (Mizuiri et al., 2005), breast (Peng et al., 2012), stomach (Shutoh et al., 2005), and colon (Wu et al., 2006). Ectopic TIG1 expression leads to cellular autophagy and suppression of growth (Shyu et al., 2016; Tsai et al., 2011).

TIG1 contains an N-terminal transmembrane domain that is structurally similar to the protein latexin. Although latexin possesses a carboxypeptidase inhibitor property, the exact role of the latexin-like domain in TIG1 remains unclear. The TIG1 gene is expressed in two isoforms, TIG1A and TIG1B, which are encoded by a 1.55-kb mRNA [GenBank: NM_206963] and an 883-bp mRNA [GenBank: NM_002888], respectively. TIG1A is predicted to encode a33.3 kDa protein with 294 amino acids and TIG1B encodes a 228-amino acid protein with a molecular weight of 25.8 kDa (Wu et al., 2011). The TIG1A isoform (NP_996846.1) shares the N-terminal 224 amino acids with TIG1B (NP_002879.2). Although TIG1A has been detected, it does not have an obviously distinct cellular function in the Wnt signaling pathway (Tsai et al., 2011) or on regulating autophagic activity (Shyu et al., 2016). In addition, previous studies examining the suppression of cell growth and invasion by TIG1 have focused on the TIG1B isoform (Jing et al., 2002; Kwok et al., 2009; Takai et al., 2005).

DnaJ heat shock protein family member C8 (DNAJC8) belongs to the heat shock protein 40 (HSP40) family, which possesses a highly conserved J-domain of approximately 70 amino acids that regulates the activity of Hsp70 proteins (Demand et al., 1998). In addition, HSP40 proteins have been shown to inhibit protein aggregation in a J-domain independent manner (Bao et al., 2002; Ito et al., 2016). Genome-wide analysis has revealed approximately 50 DnaJ/HSP40 family members in humans, although the exact number remains unclear (Qiu et al., 2006). In addition to their function as chaperones, HSP40 proteins have been reported to play an important role in cancer biology (Mitra et al., 2009; Sterrenberg et al., 2011). As a notable example of the tumor suppressor function, TID1/DNAJA3 inhibits cell proliferation, induces cancer cell apoptosis, and negatively regulates the migration of cancer cells (Cheng et al., 2005; Kim et al., 2004; 2005).

TIG1 is expressed at high levels in well-differentiated tissues. The decreased expression of TIG1 in cancer tissues suggests that TIG1 might play an important role in suppressing tumor growth. TIG1A and TIG1B exhibit similar cellular activities (Shyu et al., 2016; Tsai et al., 2011; Wu et al., 2011), and only endogenous TIG1B has been detected in cervical and hepatoma-derived cancer cells (Shyu et al., 2016). In this study, TIG1B was used to represent TIG1 and used in the subsequent studies described below. Using the cytoplasmic region of TIG1 as bait, TIG1 interacted with DNAJC8 in yeast two-hybrid screening. Because HSP40 is involved in regulating glycolysis and proliferation in tumor cells (Huang et al., 2014), we hypothesized that TIG1 might regulate glucose metabolism in cells. This study revealed the molecular mechanisms involved in the TIG1-mediated regulation of DNAJC8 function and glucose metabolism in cancer cells. Moreover, the TIG1-DNAJC8 interaction was related to the localization of pyruvate kinase M2 (PKM2) and PKM2-mediated GLUT1 expression.

MATERIALS AND METHODS

Yeast two-hybrid screening

The pAS2-1-TIG1 vector, the HeLa cell cDNA library that was fused to the GAL4 activation domain vector pACT2, and the methods for the yeast two-hybrid screen have been described previously (Shyu et al., 2016). The yeast strain CG-1945 was co-transformed with pACT2-DNAJC8 and pAS2-1-TIG1 and the transformed yeast cells were grown on a yeast dropout media lacking the indicated selection components. Samples were incubated at 30℃ for 5 days.

Expression vectors

The vectors pWZL Neo Myr Flag PKM2 and pEGFP-C1-PKM2 were purchased from Addgene (plasmid #20585 and plasmid #64698, deposited by Jean Zhao and Axel Ullrich, respectively). The Glut1 promoter reporter clone (pEZX-PG02.1-Glut1) was purchased from Genecopoeia (USA). The pTIG1-myc vector has been described previously (Wu et al., 2011). The DNAJC8 cDNA fragment was amplified from pDNAJC8/PACT2 using 5′ (5′-TGGCTAGCATGGCGGCTTCA GGAGAGAGC-3′) and 3′ (5′-GACTCGAGCTCACGTTGCTCC ATTTTTACTTTCGG-3′) primers and then was subcloned in-frame into the *Nhe*I-*Xho*I sites of PCR3.1-Flag (Dr. Yi-Ling Lin, Institute of Biomedical Science, Academia Sinica, Taiwan) to generate pDNAJC8-Flag. The DNAJC8 cDNA fragment was amplified from pDNAJC8-Flag using 5′ (5′-TCGAATTCTATGG CGGCTTCAGGAG-3′) and 3′ (5′-GTGGATCCCTCACGTTGCT CCATTTTTA-3′) primers and then subcloned in-frame into the *Eco*RI-*Bam*HI sites of the pEGFP-C1 vector (Clontech Laboratories, USA) to generate pEGFP-DNAJC8. The PKM2 cDNA fragment was amplified from pWZL Neo Myr Flag PKM2 using 5′ (5′-TCGAATTCGATGTCGAAGCCCCATAGTG-3′) and 3′ (5′-GTGGATCC CGGCACAGGAACAACACGC-3′) primers and then subcloned in-frame into the *Eco*RI-*Bam*HI sites of the pcDNA-myc-His vector (Invitrogen, USA) to generate pPKM2-myc.

Cell culture, transfection and luciferase assay

HeLa Tet-off (HtTA) cervical cancer cells were maintained in Dulbecco's Modified Eagle's Medium supplemented with 10% fetal bovine serum (FBS), 2 mM L-glutamine, 100 units/ml penicillin, and 10 μg/ml streptomycin at 37℃ under 5% CO_2 in a 95% humidified atmosphere. Cells plated in culture dishes were transfected with the expression vectors using liposome-mediated transfection. Briefly, plasmids and Lipofectamine 2000 (Gibco BRL, USA) were diluted in Opti-

MEM medium and then mixed with plasmids at room temperature for 15 min. The DNA-Lipofectamine complexes were then added to cells and incubated for 5 h at 37℃. Fresh DMEM medium containing 1% FBS was added to cells and incubated for 24-96 h at 37℃ until further analysis. Cell viability was determined using the trypan blue exclusion assay. Luciferase activity was measured using the luciferase assay kit (Stratagene, USA) and a multi-functional microplate reader (Infinite F200, Tecan, USA).

Immunoprecipitation and western blotting

For co-immunoprecipitation, HtTA cells were transfected with the indicated plasmids for 24 h. Cells were lysed with modified RIPA buffer (20 mM Tris [pH 7.5], 100 mM NaCl, 1% NP-40, and 30 mM sodium pyrophosphate) containing a protease inhibitor cocktail (Roche Diagnostics, Germany) and phosphatase inhibitors. Cell lysates were incubated with the indicated antibodies at 4℃ overnight and then incubated for 2 h at 4℃ with 20 μl of Protein G plus/Protein A-agarose (Calbiochem, USA). Immunoprecipitated complexes were analyzed by western blotting using the appropriate primary antibodies after the complexes were washed three times with modified RIPA buffer. For western blotting, 20-60 μg of proteins were separated on 12% SDS-PAGE gels and transferred to polyvinylidene fluoride membranes. After the membranes were blocked, they were incubated with anti-MYC (Invitrogen), anti-FLAG (Sigma, USA), anti-TIG1 (Santa Cruz Biotechnology, USA), anti-DNAJC8 (Thermo Fisher Scientific, USA), anti-HSP40 (Santa Cruz Biotechnology), anti-GAPDH (Cell Signaling Technology, USA), anti-Lamin B1 (Invitrogen), anti-PKM2 (Santa Cruz Biotechnology), anti-Glut1 (Santa Cruz Biotechnology), or anti-Actin (Sigma) antibodies for 12 h at 4℃ and then incubated with a horseradish peroxidase-conjugated goat anti-mouse antibody for 1 h at room temperature. An ECL kit (Amersham, UK) was used to detect the labeled antibodies.

Cell fractionation

The TIG1, DNAJC8 and PKM2 distributions in cells were analyzed using the Qproteome Cell Compartment Kit (Qiagen, USA), according to the manufacturer's instructions. Protease and phosphatase inhibitors were added to all buffers. Cells were scraped and washed with cold PBS twice. The cytosolic and nuclear fractions were obtained from centrifuged cell pellets that had been incubated with the extraction buffers at 4℃. The proteins in the cell fraction were detected by SDS-PAGE and immunoblotting.

Immunofluorescence analysis

HtTA cells (1×10^5) were plated on poly-L-lysine-coated coverslips in 35-mm dishes and cultured with growth medium. Cells were then transfected with 500 ng of the indicated expression vector for 18 h. Cells were washed and fixed with 4% paraformaldehyde and then analyzed using a Leica TCS SP5 scanner (Leica, Germany).

Glucose uptake and lactate production measurements

Cells were cultured on 6-well plates overnight and then transfected with the indicated expression vector or siRNA for 24 h. The medium was collected to detect glucose uptake and lactate production. Glucose uptake was measured using the glucose assay kit (Sigma), and lactate production was measured using the lactate assay kit (Abcam, UK).

RNA interference

TIG1 siRNAs, which target nucleotides 488-508 of TIG1, have been described previously (Wu et al., 2011). DNAJC8 and PKM2 siRNA oligonucleotides were synthesized by Sigma. The DNAJC8 siRNA targeting nucleotides 885-903 (5'-CAUAGAGUAGUAUUUGCUUtt-3'), the Glut1 siRNA targeting nucleotides 902-920 (5'-GCUUCAUCAUCGGUGUGUAtt-3'), and the PKM2 siRNA targeting nucleotides 1047-1065 (5'- CGUGGAUGAUGGGCUUAUUtt-3') were synthesized based on GenBank accession numbers NM_014280.2, NM_006516.2, and NM_002654, respectively. The universal control (NC) siRNA (Sigma) was used as a negative control.

RNA isolation and quantitative real-time reverse transcription PCR

The total RNA was extracted from cells using Trizol (Invitrogen), and cDNAs were prepared using M-MLV reverse transcriptase (Invitrogen) and oligo $(dT)_{12-18}$. Quantitative real-time PCR (Q-PCR) was performed in triplicate using 20 μl of a reaction mixture containing 10 μl of Fast SYBR Green Master Mix (ABI, Applied-Biosystems, USA), 50 ng of cDNAs, and gene-specific forward and reverse primers at a 1 μM final concentration in a thermal cycler (7900HT Fast Real-Time PCR System, ABI). The PCR cycling program consisted of an initial incubation at 95℃ for 3 min, 40 cycles of denaturation at 95℃ for 15 s and annealing and extension at 60℃ for 1 min. The PCR primers used for amplification included the following: β-actin (sense, 5'-TCCCTGGAGAAGAGCTACG-3' and antisense, 5'-GTAGTTTCGTGGATGCCACA-3'), Glut1 (sense, 5'-TGGCATCAACGCTGTCTTCT-3' and antisense, 5'-CTAGCGCGATGGTCATGAGT-3'), Glut2 (sense, 5'-TTGAAGCCACAGGTTGCTGA-3' and antisense, 5'-AGGGTCCCAGTGACCTTATCT-3'), Glut3 (sense, 5'-TCCACCCTTTGCGGAGATTAT-3' and antisense, 5'-TGGGGTGACCTTCTGTGTC-3'), and Glut4 (sense, 5'-ACTGGCCATTGTTATCGGCA-3' and antisense, 5'-GTCAGGCGCTTCAGACTCTT-3'). The relative expression levels of the target cDNAs were calculated after normalizing the relative intensity of the target cDNA to the intensity of β-actin.

Statistical analysis

The data are presented as means ± SD of at least triplicate experiments. Statistical analyses were performed using one-way ANOVA with Dunnett's post hoc test for comparisons of more than two groups. Student's t test was used to compare differences between two groups. A p-value < 0.05 was considered statistically significant.

RESULTS

TIG1 interacts with DNAJC8, and the proteins are co-localized in the cytosol

The yeast-two hybrid system was used to screen for potential proteins that interacted with TIG1 to identify the regulatory

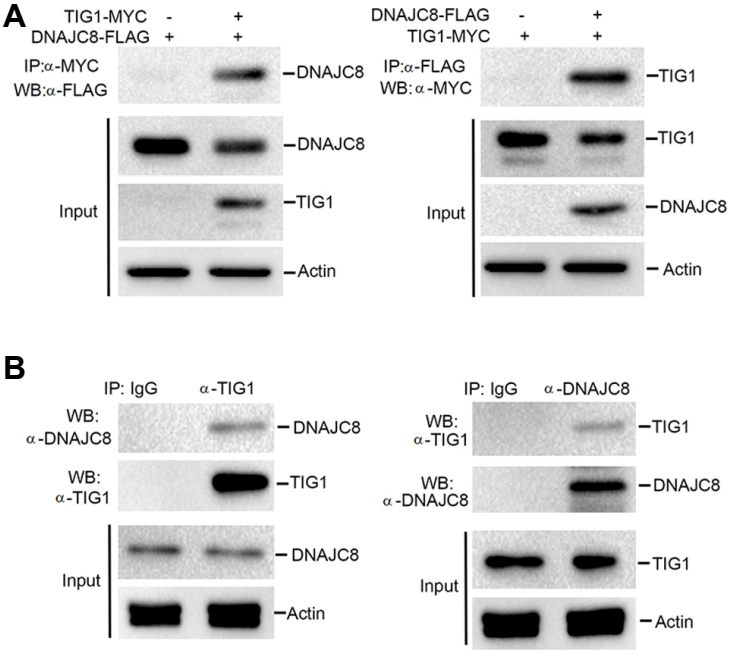

Fig. 1. TIG1 interacts with DNAJC8. Lysates of HtTA cells co-transfected with TIG1-myc and the DNAJC8-flag expression vector were immunoprecipitated with the anti-MYC antibody or anti-FLAG antibody, and the bound proteins were detected using FLAG antibody or anti-MYC antibody. The levels of total DNAJC8, TIG1, and Actin in the cytosolic extracts were detected by western blotting (A). HtTA cell lysates were prepared, and the interaction between TIG1 and DNAJC8 was analyzed by immunoprecipitation using anti-TIG1 or anti-DNAJC8 antibodies, respectively, followed by western blot analysis (B). HtTA cells were cotransfected with EGFP-DNAJC8 and TIG1-myc expression vectors for 18 h. Cells were fixed and then incubated with the anti-MYC antibody followed by Alexa Fluor 488-conjugated goat anti-mouse IgG or Alexa Fluor 633-conjugated goat anti-mouse IgG antibodies. Cells were then stained with DAPI and analyzed with a laser scanning confocal microscope. Scale bar: 10 μm (C).

mechanism by which TIG1 suppresses cancer. DNAJC8 was identified in the pool, and both the DNAJC8 prey vector and TIG1 bait vector were required for yeast growth in nutrient-deficient medium, suggesting that DNAJC8 interacted with TIG1 (Supplementary Fig. S1). We first constructed expression vectors that synthesized recombinant proteins containing Flag-tagged DNAJC8 to further confirm the interaction between TIG1 and DNAJC8. Overexpression and co-immunoprecipitation assays were performed to confirm the interaction between DNAJC8 and TIG1 in HtTA cancer cells. DNAJC8 and TIG1 proteins interacted when they were both overexpressed in HtTA cells (Fig. 1A). The endogenous TIG1-DNAJC8 interaction was also confirmed by reciprocal co-immunoprecipitation in the HtTA cell lysates (Fig. 1B). We next analyzed the subcellular localization of these proteins to further examine the distribution of the TIG1 and DNAJC8 proteins in cells. EGFP-DNAJC8 was predominantly localized in the nucleus and had a partial distribution in the cytosol. The TIG1 protein, however, was localized in the perinuclear region. The nuclear localization of EGFP-DNAJC8 was markedly reduced in cells co-expressing TIG1, and DNAJC8 colocalized with TIG1 in the perinuclear region (Fig. 1C). Based on these data, both TIG1 and DNAJC8 are localized in the perinuclear region and interact with each other.

TIG1 alleviates the DNAJC8-induced increase in glucose consumption and lactate production

The effect of TIG1 on DNAJC8 expression in transiently transfected HtTA cells was analyzed by western blotting. DNAJC8 levels were reduced in a dose-dependent manner,

with a maximal 34.6% reduction in cells transfected with 5 μg of the TIG1 expression vector (Fig. 2A). The decreased endogenous DNAJC8 expression was also observed in cells expressing TIG1. However, the level of HSP40 was not affected when cells were transfected with the TIG1 expression vector (Supplementary Fig. S2). Similarly, DNAJC8 expression decreased the levels of the TIG1 protein, and the maximal suppression of 30.5% occurred in cells that had been transfected with 5 μg of the DNAJC8 expression vector (Fig. 2B). Based on immunofluorescence assay results, the DNAJC8 protein was present only in the perinuclear region when cells expressed the TIG1 protein (Fig. 1C). The distribution of the TIG1 and DNAJC8 proteins was detected by cell fractionation to examine whether TIG1 expression affected the subcellular localization of DNAJC8. TIG1 was mainly detected in the cytosolic fraction of HtTA cells transfected with the TIG1 expression vector, whereas DNAJC8 was mainly detected in the nuclear fraction in cells expressing DNAJC8. The levels of nuclear DNAJC8 in TIG1-expressing cells were profoundly decreased compared with cells that only expressed the DNAJC8 protein (Fig. 2C). Thus, the interaction with TIG1 facilitated the translocation of DNAJC8 to the cytosol.

HSP40 has been shown to regulate glycolysis and proliferation in cancer cells (Huang et al., 2014). The regulatory effects of DNAJC8 and TIG1 on glycolysis were further examined. HtTA cells expressing DNAJC8 displayed higher glucose consumption than control cells. Decreased glucose consumption was observed in cells co-expressing TIG1 and DNAJC8 compared with DNAJC8-expressing cells (Fig. 2D). Similarly, lactate production was dramatically increased in cells expressing DNAJC8, whereas the elevated lactate production was inhibited when cells were co-transfected with the pDNAJC8-Flag and pTIG1-myc expression vectors (Fig. 2E). Cells that expressed TIG1 alone did not exhibit significant

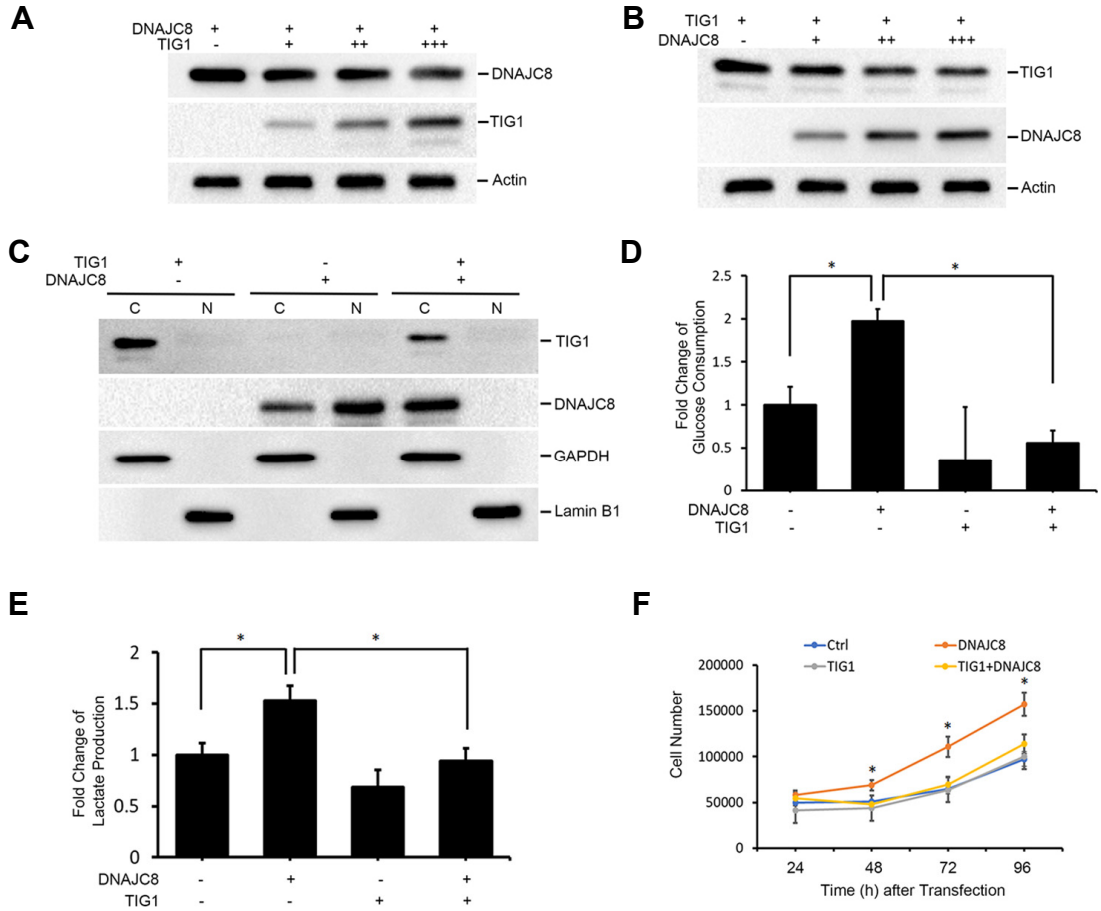

Fig. 2. TIG1 inhibits DNAJC8 expression and the DNAJC8-mediated increase in glycolysis. Lysates were prepared from HtTA cells transfected with 0.5 μg (A) or 0.5-1.5 μg (B) of DNAJC8-flag expression vector along with 0.5-1.5 μg (A) or 0.5 μg (B) of TIG1-myc expression vector. The levels of TIG1, DNAJC8, and Actin were determined by immunoblotting. The nuclear and cytosolic fractions of HtTA cells transfected with TIG1-myc and DNAJC8-flag vectors were prepared, and the levels of TIG1 and DNAJC8 were determined by immunoblotting. GAPDH and Lamin B1 were markers of the cytosolic and nuclear fractions, respectively (C). The media were collected from HtTA cells transfected with TIG1-myc and DNAJC8-flag vectors, and glucose consumption (D) and lactate production (E) were determined using enzyme immunoassays. HtTA cells were transfected with TIG1-myc and DNAJC8-Flag vectors, and the cell numbers were counted at 24 to 96 h (F).

changes in glucose consumption and lactate production. Since glucose consumption and lactate production were significantly increased in cells expressing DNAJC8, we next examined the effect of DNAJC8 on cell proliferation. As shown in Fig. 2F, HtTA cells expressing DNAJC8 grew faster than control cells. The increase in cell growth was abolished when HtTA cells co-expressed TIG1 and DNAJC8 (Fig. 2F).

Similar results were observed in HCT116 colorectal cancer cells, for which DNAJC8 alone was primarily distributed in the nuclear fraction, but most of the DNAJC8 was present in the cytosolic fraction in the presence of TIG1 (Supplementary Fig. S3A). Consistent with the results of the cell fractionation assay, TIG1 and EGFP-DNAJC8 proteins were co-localized in co-transfected HCT116 cells (Supplementary Fig. S3B). Similar results for glucose consumption, lactate production, and cell proliferation were observed in HCT116 cells expressing TIG1 and DNAJC8 (Supplementary Figs. S3C-S3E).

The growth rates of HtTA cells grown in medium supplemented with galactose were slower than were those of cells grown in medium supplemented with glucose. No significant change in cell growth was observed in cells expressing DNAJC8 or TIG1 compared with control cells in the medium supplemented with galactose, indicating that DNAJC8 promoted cell proliferation by regulating glucose metabolism (Supplementary Fig. S4).

DNAJC8 silencing suppresses glucose consumption and lactate production

RNA interference was used to investigate the effects of endogenous TIG1 and DNAJC8 on the production of the other protein. TIG1 expression was slightly increased by 32% when cells were transfected with the DNAJC8 siRNA, whereas DNAJC8 expression was increased by 17.7% in cells in which TIG1 expression was silenced (Fig. 3A). Endogenous TIG1 or DNAJC8 expression in HtTA cells was silenced to confirm the effects of TIG1 or DNAJC8 on glucose uptake. Glucose consumption and lactate production were decreased by 59.6% and 28.7%, respectively, in DNAJC8-silenced cells compared with those in control cells. By contrast, glucose uptake and lactate production were increased by 36.7% and 17.7%, respectively, in TIG1-silenced cells compared with those in control cells (Figs. 3B and 3C). DNAJC8-silenced cells exhibited a significant decrease in cell growth of 33.6% compared with the control siRNA-transfected cells (Fig. 3D). By contrast, cells transfected with TIG1 siRNA exhibited a significant increase in cell growth of 23.6%.

DNAJC8 increases GLUT1 expression

Because DNAJC8 upregulates glycolysis, we next examined whether DNAJC8 influences glycolysis by affecting the expression of glucose transporters. We measured the effect of DNAJC8 on the levels of mRNAs encoding glucose transporters in cells expressing DNAJC8. Increased expression of Glut1 mRNA, but no other Glut transporters, was observed in HtTA cells transfected with the DNAJC8 expression vectors (Fig. 4A). The Glut1 promoter report assay was further used to evaluate the DNAJC8-mediated Glut1 expression. A 3.1-fold increase in the promoter activity was observed in cells expressing DNAJC8 compared with control cells (Fig. 4B). In

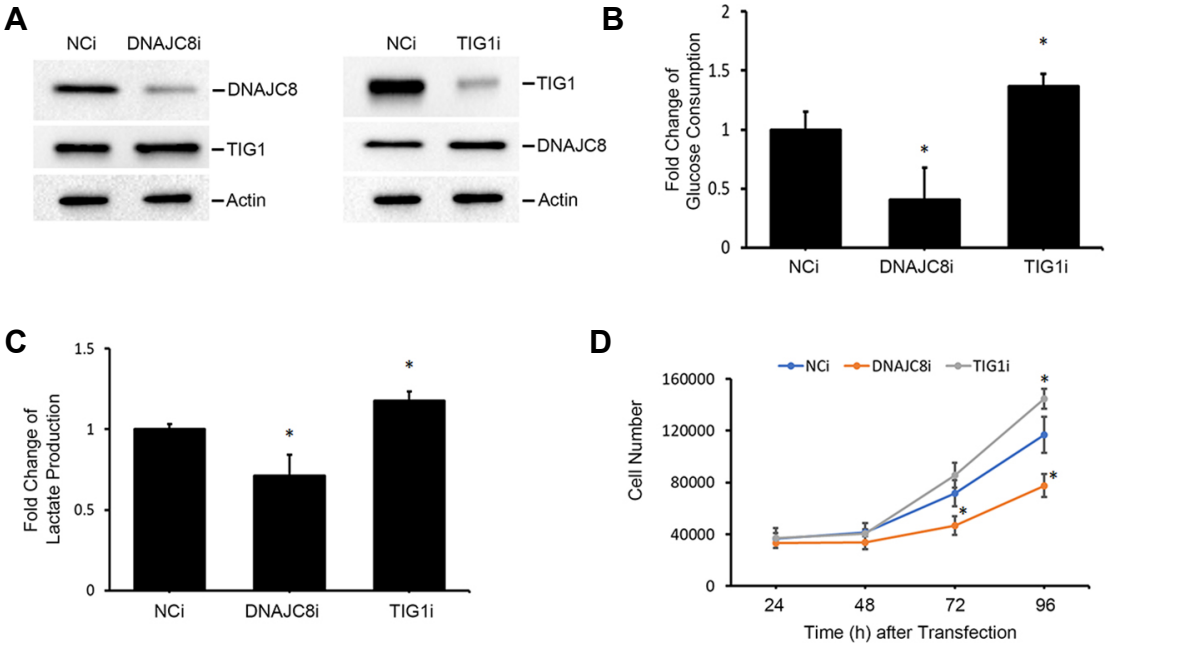

Fig. 3. Effects of TIG1 and DNAJC8 siRNAs on glycolysis. Lysates of HtTA cells transfected with negative control (NCi), TIG1 or DNAJC8 siRNA were prepared, and the levels of TIG1 and DNAJC8 were determined by immunoblotting (A). Media were collected from HtTA cells transfected with the TIG1 or DNAJC8 siRNA and glucose consumption (B) and lactate production (C) were determined using enzyme immunoassays. HtTA cells were transfected with TIG1 or DNAJC8 siRNAs and cell numbers were counted at 24 to 96 h (D).

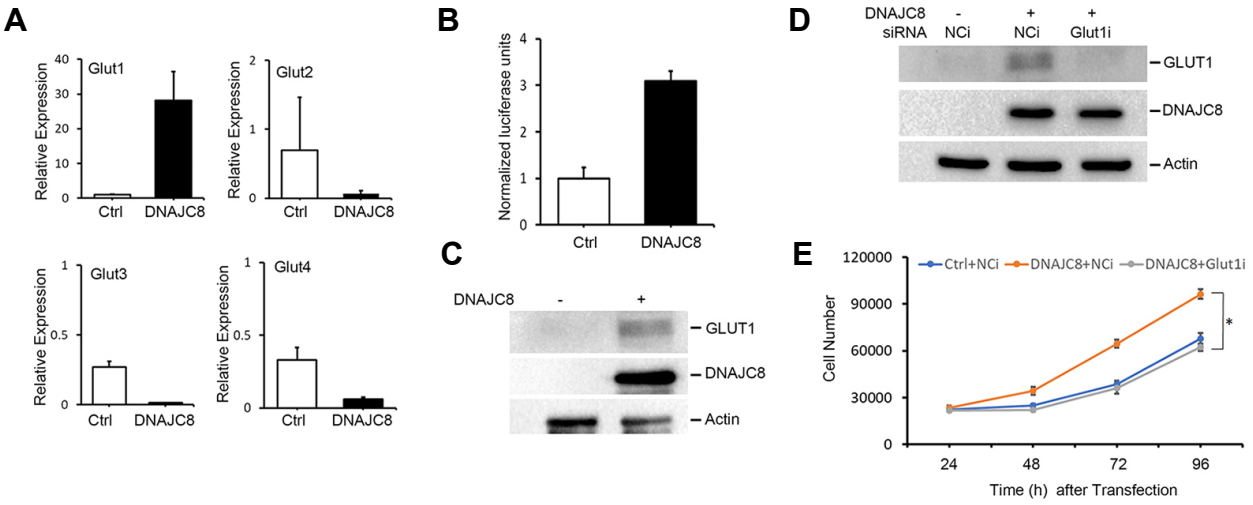

Fig. 4. DNAJC8 induces GLUT1 expression. Total RNA was extracted from HtTA cells transfected with the empty vector or DNAJC8-flag expression vector. The relative levels of the indicated mRNAs were measured by real-time RT-PCR. The data were expressed as relative expression normalized to the Glut1 mRNA expression of control cells (A). HtTA cells were plated in triplicate, incubated overnight, and then transfected with control vector, DNAJC8-flag expression vector, and Glut1 promoter reporter plasmids for 24 h. The cultured supernatants were prepared and analyzed for the activity of the Glut1 promoter. The data were expressed as relative luciferase activity normalized to that of control cells (B). Lysates were prepared from HtTA cells transfected with the empty vector or DNAJC8-flag expression vector for 24 h and the levels of GLUT1, DNAJC8, and Actin were determined by immunoblotting (C). The lysates of HtTA cells co-transfected with DNAJC8-flag and NCi or Glut1 siRNA were prepared and the levels of GLUT1, DNAJC8, and Actin were determined by immunoblotting (D). The cell numbers were counted at 24 to 96 h after the cells were co-transfected with the DNAJC8-flag vector and NCi or Glut1 siRNA (E).

addition, DNAJC8 expression increased the level of the GLUT1 protein by 3.86-fold in transfected cells (Fig. 4C), while the GLUT1 protein level induced by DNAJC8 was reduced in Glut1 siRNA-transfected cells (Fig. 4D). Furthermore, silencing of Glut1 significantly alleviated DNAJC8-mediated cell growth promotion (Fig. 4E).

PKM2 enhances DNAJC8-mediated glucose consumption and lactate production

HSP40 has been shown to interact with PKM2 and regulate glycolysis in HeLa cells (Huang et al., 2014). Because DNAJC8 and HSP40 belong to the same HSP family, we presumed that the binding of DNAJC8 to PKM2 would also be observed in HtTA cells. Co-immunoprecipitation assays were performed to confirm the interaction between DNAJC8 and PKM2. DNAJC8 and PKM2 proteins interacted with each other when both were overexpressed in HtTA cells (Fig. 5A). We further verified the subcellular localization of DNAJC8 and PKM2 proteins within cells. The EGFP-PKM2 protein was dispersed in the cytosol, whereas DNAJC8 was predominantly localized in the nucleus. As shown in Fig. 5B, the distribution of EGFP-PKM2 was markedly shifted to the nucleus of cells co-expressing DNAJC8 and EGFP-PKM2, where it colocalized with DNAJC8. Based on the result of the cell fractionation assay, PKM2 was present in the cytosolic fraction. However, PKM2 was observed in cell nuclei in cells co-expressing DNAJC8 and PKM2 (Fig. 5C). Thus, DNAJC8 might interact with PKM2 and facilitate the translocation of PKM2 to the nucleus.

The translocation of PKM2 to the cell nucleus had been shown to promote GLUT1 expression (Salani et al., 2015; Yang and Lu, 2013; Yang et al., 2012). PKM2 overexpression enhanced DNAJC8-mediated GLUT1 expression by 18.6% (Fig. 5D). Furthermore, glucose consumption and lactate production were increased by 54% and 30.4%, respectively, in cells with co-transfected DNAJC8 and PKM2 expression vectors compared with cells expressing DNAJC8 alone (Figs. 5E and 5F). The GLUT1 levels, glucose consumption and lactate production were not changed in cells transfected with the PKM2 expression vector alone. However, PKM2 overexpression increased the growth of cells co-expressing DNAJC8 and PKM2 compared with cells expressing DNAJC8 alone (Fig. 5G).

Silencing of PKM2 expression alleviates DNAJC8-mediated glucose consumption and lactate production

We examined the effects of PKM2 silencing on GLUT1 expression, glucose consumption, and lactate production in DNAJC8-expressing cells to investigate the role of PKM2 in the DNAJC8-mediated increase in glycolysis. Compared with control cells, the level of the GLUT1 protein was increased by 2.9-fold in cells transfected with the DNAJC8 expression vector. The levels of DNAJC8-stimulated GLUT1 expression were 30.3% lower in PKM2-silenced cells than they were in cells transfected with the negative control siRNA (Fig. 6A). Glucose consumption and lactate production were increased by 105% and 63%, respectively, in cells transfected with the DNAJC8 expression vector and negative control siRNA (Figs.

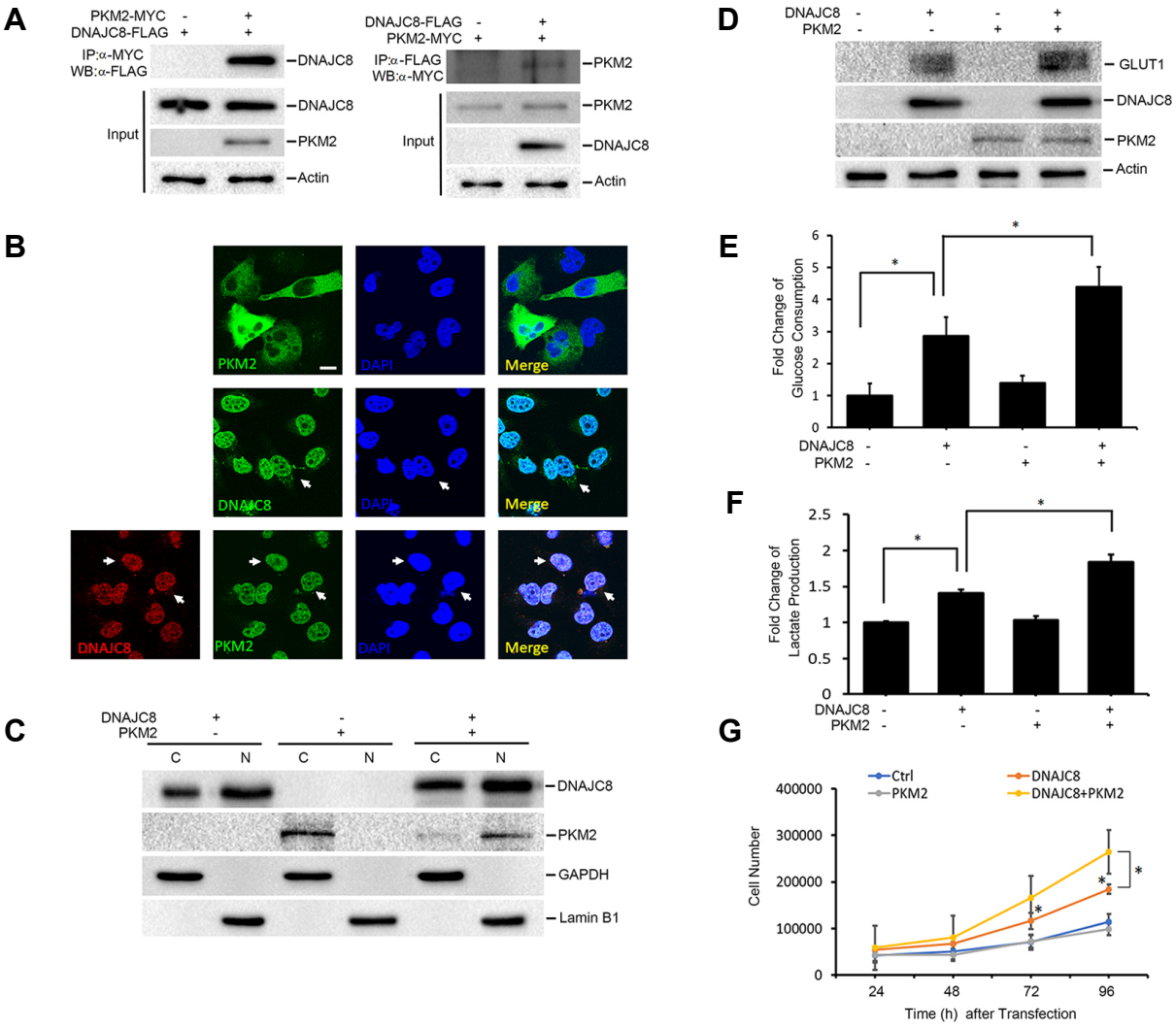

Fig. 5. DNAJC8 interacts with PKM2, and PKM2 enhances the DNAJC8-mediated increase in glycolysis. Lysates of HtTA cells co-transfected with the PKM2-myc and DNAJC8-flag expression vectors were immunoprecipitated with the anti-MYC antibody or anti-FLAG antibody. Bound proteins were detected with a FLAG antibody or anti-MYC antibody. The levels of total DNAJC8, PKM2, and Actin in the cytosolic extracts were detected by western blotting (A). HtTA cells were cotransfected with EGFP-PKM2 and DNAJC8-flag expression vectors for 18 h. Cells were fixed and then incubated with an anti-FLAG antibody followed by Alexa Fluor 488-conjugated goat anti-mouse IgG or Alexa Fluor 633-conjugated goat anti-mouse IgG antibodies. Cells were then stained with DAPI and analyzed using a laser scanning confocal microscope. Scale bar: 10 μm (B). Nuclear and cytosolic fractions of HtTA cells transfected with PKM2-myc and DNAJC8-flag were prepared and the levels of PKM2 and DNAJC8 were determined by immunoblotting (C). The lysates of HtTA cells transfected with PKM2-myc and DNAJC8-flag expression vectors were prepared and the levels of GLUT1, DNAJC8, PKM2, and Actin were determined by immunoblotting (D). The media were collected from HtTA cells transfected with the PKM2-myc or DNAJC8-flag expression vector and glucose consumption (E) and lactate production (F) were determined using enzyme immunoassays. HtTA cells were transfected with the PKM2-myc or DNAJC8-flag expression vector and the cell numbers were counted at 24 to 96 h (G).

6B and 6C). Glucose consumption and lactate production were markedly decreased by 41.2% and 26.9%, respectively, in DNAJC8-expressing cells transfected with the PKM2 siRNA compared with cells transfected with the negative control siRNA (Figs. 6B and 6C). In addition, silencing PKM2 expression significantly alleviated DNAJC8-mediated cell growth (Fig. 6D).

TIG1 decreases DNAJC8-mediated PKM2 nuclear translocation

Based on our results, PKM2 is important to promote DNAJC8-mediated glycolysis. We proposed that the TIG1-DNAJC8 interaction would change the localization of PKM2 within cells and subsequently affect PKM2-mediated GLUT1 expression. PKM2 was transfected into the DNAJC8 or DNAJC8 and TIG1 co-overexpressing cells to confirm this

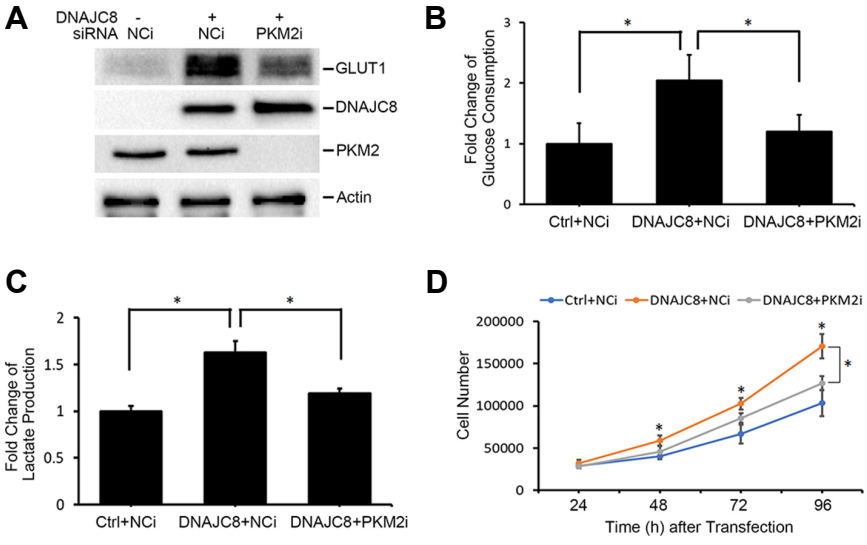

Fig. 6. PKM2 siRNA alleviates the DNAJC8-mediated increase in glycolysis. The lysates of HtTA cells co-transfected with DNAJC8-flag and the NCi or PKM2 siRNA were prepared and the levels of GLUT1, DNAJC8, PKM2, and Actin were determined by immunoblotting (A). The media were collected from HtTA cells co-transfected with the DNAJC8-flag expression vector and NCi or PKM2 siRNA, and the glucose consumption (B) and lactate production (C) were determined using enzyme immunoassays. The cell numbers were counted at 24 to 96 h after cells were co-transfected with the DNAJC8-flag vector and NCi or PKM2 siRNA (D).

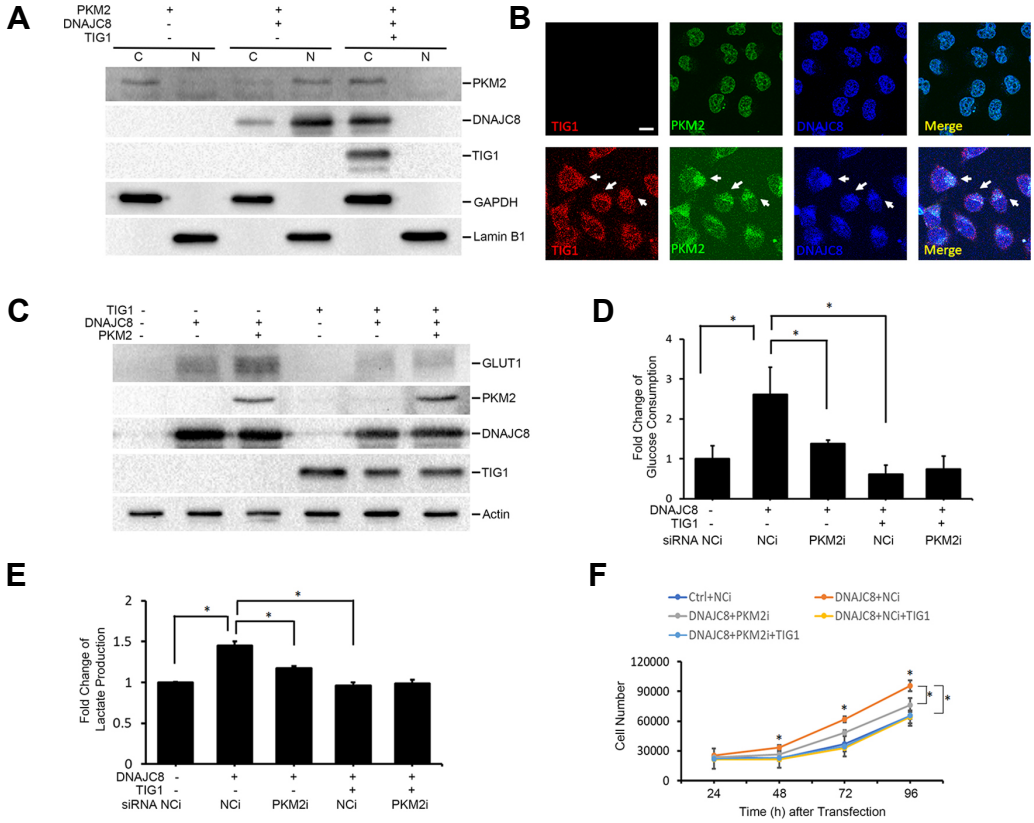

Fig. 7. TIG1 inhibits DNAJC8-mediated PKM2 translocation. Nuclear and cytosolic fractions were prepared from HtTA cells transfected with TIG1-myc, PKM2-myc, and DNAJC8-flag, and the levels of TIG1, PKM2, and DNAJC8 were determined by immunoblotting (A). HtTA cells were cotransfected with EGFP-PKM2, DNAJC8-Flag, and TIG1-myc expression vectors for 18 h. Cells were fixed and then incubated with anti-MYC and anti-DNAJC8 antibodies, followed by Alexa Fluor 633-conjugated goat anti-mouse IgG and Alexa Fluor 405-conjugated goat anti-rabbit IgG antibodies. Cells were then analyzed using a laser scanning confocal microscope. Scale bar: 10 μm (B). Lysates of HtTA cells transfected with TIG1-myc, PKM2-myc, and DNAJC8-flag vectors were prepared, and the levels of GLUT1, PKM2, DNAJC8, TIG1, and Actin were determined by immunoblotting (C). The media were collected from HtTA cells co-transfected with DNAJC8-flag and TIG1-myc expression vectors along with the NCi or PKM2 siRNA, and glucose consumption (D) and lactate production (E) were determined using enzyme immunoassays. Cell numbers were counted at 24 to 96 h after cells were transfected with the DNAJC8-flag and TIG1-myc expression vectors along with the NCi or PKM2 siRNA (F).

hypothesis. The distribution of the PKM2 protein was determined using cell fractionation. In the control cells, PKM2 was largely detected in the cytosolic fraction. The level of nuclear PKM2 in DNAJC8-expressing cells was increased by 39.9% compared with control cells. This increase was abolished by TIG1 expression (Fig. 7A). A similar result was observed for EGFP-PKM2, which was predominantly distributed in the cytosol of HtTA cells co-expressing TIG1 and DNAJC8 compared with the nuclear distribution of EGFP-PKM2 in cells expressing DNAJC8 alone (Fig. 7B). Increased PKM2 expression enhanced the DNAJC8-mediated increase in the GLUT1 protein level, and the elevated GLUT1 protein level was decreased by 86.2% in cells co-expressing DNAJC8 and TIG1 (Fig. 7C).

Our results showed a partial, but significant, reversion of DNAJC8-mediated upregulation of glycolysis in DNAJC8-expressing HtTA cells after transfection with the PKM2 siRNA. The PKM2 siRNA was transfected into TIG1-expressing cells to evaluate the role of PKM2 in TIG1-mediated suppression of DNAJC8-induced glycolysis. Silencing of PKM2 expression significantly alleviated the DNAJC8-mediated increase in glucose consumption and lactate production by 47.1% and 18.8%, respectively (Figs. 7D and 7E). Cells expressing TIG1 exhibited complete inhibition of the DNAJC8-induced increase in glucose consumption and lactate production, whereas PKM2 siRNA had no effect on the glucose consumption and lactate production in TIG1 and DNAJC8 co-expressing cells (Figs. 7D and 7E). Based on these findings, PKM2 participates in DNAJC8-mediated signaling pathways in the nucleus. These results may explain the lack of a further effect of PKM2 silencing when DNAJC8 was translocated to the cytosol through its interaction with TIG1. In addition, TIG1 expression completely abolished DNAJC8-induced cell growth. PKM2 silencing had no effect on the growth of TIG1 and DNAJC8 co-expressing HtTA cells, although transfection of the PKM2 siRNA partially reduced the growth of DNAJC8-expressing cells (Fig. 7F).

Because TIG1 is a retinoid-inducible protein (Nagpal et al., 1996; Shyu et al., 2016), we also examined whether all-trans retinoic acid (ATRA) contributes to DNAJC8-mediated regulation of glucose metabolism. Higher glucose consumption and lactate production was observed in cells expressing DNAJC8 compared with control cells. However, either glucose consumption or lactate production was not affected in DNAJC8-expressing cells treated with ATRA compared with control cells (Supplementary Fig. S5).

DISCUSSION

DNAJC8 interacted with PKM2 to affect its localization in cells and subsequently induced Glut1 expression to further facilitate glucose uptake. As a result, cancer cell proliferation was impacted by DNAJC8 via the PKM2 protein (Fig. 8, left panel). The nuclear translocation of PKM2 is a prerequisite for its effect on enhancing Glut1 expression. However, the expression of TIG1 retains DNAJC8 in the cytosol, diminishes PKM2 accumulation in the cell nucleus and reduces the cells' capability to enhance glucose metabolism induced by DNAJC8 (Fig. 8, right panel). Cells expressing TIG1 alone did

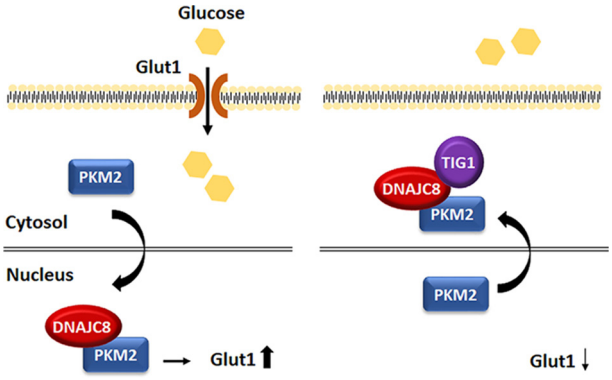

Fig. 8. Schematic model of the mechanism by which TIG1 inhibits the DNAJC8-mediated increase in glycolysis through PKM2 translocation. DNAJC8 binds to PKM2 and induces its accumulation in the cell nucleus, thereby inducing Glut1 expression to promote glucose uptake. TIG1 interacts with DNAJC8 in the cytosol and subsequently inhibits DNAJC8-mediated PKM2 translocation.

not induce significant changes in glucose uptake and cell proliferation, even ectopic TIG1 suppressed endogenous DNAJC8 expression (Fig. 2 and Supplementary Fig. S2). Although HSP40 was not affected by TIG1, redundant DNAJC8 expression might be the main cause of the minor effect of ectopic TIG1 expression on glucose metabolism. Regardless of the minor effect of ectopic TIG1 on glucose metabolism, TIG1 silencing significantly induced glucose uptake and the cell population (Fig. 3).

In the present study, we observed a complete reversion of DNAJC8-mediated growth enhancement in DNAJC8-expressing cells after transfection with Glut1 siRNA (Fig. 4E). This result indicated that GLUT1 is a major contributor to participate in DNAJC8-regulated induction of glucose metabolism. By contrast, knockdown of PKM2 expression did not completely abolish the DNAJC8-mediated increase in glycolysis, suggesting that other unknown transcription factors are present in the nucleus in addition to PKM2 and may potentially participate in DNAJC8-mediated Glut1 expression (Fig. 6). The phenomenon was confirmed because DNAJC8 was translocated to the cytosol through its interaction with TIG1; thus DNAJC8 lost its ability to enhance glycolysis (Fig. 7).

HSPs are a group of proteins that are upregulated when cells are exposed to stressful conditions, such as elevated temperatures or oxygen deprivation. Many HSPs perform chaperone functions by ensuring that target proteins are in the proper conformation or location (Whitley et al., 1999). Various diseases may create a challenging environment and induce various stress responses that sequentially induce the production of HSPs. Therefore, the reported involvement of HSPs in various types of cancers is not surprising. Regardless of the cause or result for cancer cell development, HSPs are diagnostic, prognostic, or predictive markers for cancer (Ciocca and Calderwood, 2005). A study of patients with lung cancer showed an overexpression of HSP40 in human tumor tissues and the concomitant presence of HSP40 auto-

antibodies in the serum (Oka et al., 2001). HSP27 has been reported to be involved in cell migration, cell growth, differentiation, and tumor progression, and HSP27 overexpression has been observed in prostate cancer, breast cancer, and brain tumors (Assimakopoulou, 2000; Banerjee et al., 2011; Miyake et al., 2006). As shown in the study by Hwang et al., HSP60 expression is upregulated in cervical cancer (Hwang et al., 2009). Moreover, in patients with colon cancer or breast cancer, the overexpression of HSP60 is significantly correlated with the cancer grade and may also have an important prognostic impact on the survival rate of patients (Hamelin et al., 2011; Hamrita et al., 2008). In several cancers, HSP70 overexpression is correlated with an increased cell proliferation rate and malignancy (Guo et al., 2005; Maehara et al., 2000; Murphy, 2013; Yoshidomi et al., 2014).

Little information about the relationship between cancer development and DNAJC8 expression is available in the literature. In contrast to the findings from our study, overexpression of the DNAJC8 homolog HSP40/DNAJB1 in HeLa cells negatively regulates PKM2 activity and suppresses glycolysis metabolism (Huang et al., 2014). This observation suggests that different HSPs may exhibit opposite biological activities. Similar results were observed for Tid1/DNAJA3 because the long form of Tid1/DNAJA3 promotes cell apoptosis and the short form of TID1/DNAJA3 suppresses cell death (Edwards and Munger, 2004; Syken et al., 1999). Moreover, various HSP40 members have been shown to both promote and suppress cancer development (Mitra et al., 2009; Sterrenberg et al., 2011). Overall, this review of the literature combined with the results of previous reports (Huang et al., 2014) and our own current studies suggests that the roles of members of the HSP40 family in cancer development are important and may lead to discoveries of novel signaling pathways and targets for the treatment of cancers.

Multiple roles of ATRA in growth, vision, reproduction, epithelial cell differentiation, and immune function have been discussed (Clagett-Dame and DeLuca, 2002; Degos et al., 1995; Siddikuzzaman et al., 2011; Yan et al., 2016). The actions of ATRA are mediated by the nuclear retinoid receptors that enhance the transcription of target genes by binding to retinoic acid response elements in the promoter region of retinoid-responsive genes. ATRA has been shown to stimulate glucose uptake via the AMP-activated protein kinase pathway/Rac1 in skeletal muscle cells (Lee et al., 2008). Although TIG1 is one of ATRA-induced genes (Nagpal et al., 1996), TIG1 may not completely reflect the biological effect of ATRA on glucose metabolism due to multiple effectors affected by ATRA. This may explain the not statistically significant reversion of DNAJC8-induced glucose uptake and lactate production in DNAJC8 expressing cells treated with ATRA compared with that in control cells (Supplementary Fig. S5).

TIG1 is considered a tumor suppressor. TIG1 inhibits cell invasiveness and cell proliferation, induces cellular apoptosis in vitro (Jing et al., 2002; Kwok et al., 2009; Tsai et al., 2011; Wu et al., 2011), and suppresses tumorigenicity in vivo (Jing et al., 2002). In addition, TIG1 is expressed at significantly lower levels in hepatocellular carcinoma, prostate cancer, and poorly differentiated colorectal adenocarcinomas than it is in adjacent normal tissues (Chen et al., 2014; Jing et al., 2002; Wu et al., 2006). In inflammatory breast cancer, however, the depletion of TIG1 decreases cancer cell proliferation, migration, and invasion and inhibits tumor growth (Wang et al., 2013). Based on these observations, TIG1 has multiple functions in various tissues, and the identification of different signaling pathways involved in TIG1-mediated regulation of the progression of cancer development might be due to the differences in TIG1-binding proteins in different cells. For example, TIG1 has been reported to interact with and stabilize Axl in breast cancer cells, enhancing the expression of matrix metalloproteinase-9 and activating the NF-κB signaling pathway, subsequently increasing cell invasion (Wang et al., 2013). By contrast, enhanced autophagic activity via transmembrane protein 192 has been observed during the TIG1-mediated death of cervical and hepatoma-derived cancer cells (Shyu et al., 2016). Similarly, as shown in the present study, TIG1 suppressed the DNAJC8-mediated increase in glycolysis. Because the regulatory effects of TIG1 on glycolysis depend on DNAJC8, the correlation between cancer progression and DNAJC8 expression requires further investigation. Moreover, additional analyses of the localization of TIG1 and DNAJC8 and expression of each protein in clinical specimens should be performed. The results will be useful for identifying the possible mechanism by which TIG1 regulates glycolysis through its interaction with DNAJC8.

In summary, our findings provide insights into the molecular mechanism by which TIG1 suppresses DNAJC8 expression, thus regulating cancer cell glycolytic metabolism partially by affecting PKM2 translocation. PKM2 regulates glycolysis to promote cancer cell proliferation, and the finding that TIG1 interacts with DNAJC8 to mediate PKM2 translocation may offer new targets for treatments designed to prevent cancer cell growth.

Note: Supplementary information is available on the Molecules and Cells website (www.molcells.org).

ACKNOWLEDGMENTS

This work was supported by a grant (TCRD-TPE-105-17) from the Taipei Tzuchi Hospital through the Buddhist Tzuchi Medical Foundation, Taipei, Taiwan. The authors thank the Core Laboratory of the Buddhist Tzuchi General Hospital for support.

REFERENCES

Assimakopoulou, M. (2000). Human meningiomas: immunohistochemical localization of progesterone receptor and heat shock protein 27 and absence of estrogen receptor and PS2. Cancer Detect. Prev. *24*, 163-168.

Banerjee, S., Lin, C.F., Skinner, K.A., Schiffhauer, L.M., Peacock, J., Hicks, D.G., Redmond, E.M., Morrow, D., Huston, A., Shayne, M., et al. (2011). Heat shock protein 27 differentiates tolerogenic macrophages that may support human breast cancer progression. Cancer Res. *71*, 318-327.

Bao, Y.P., Cook, L.J., O'Donovan, D., Uyama, E., and Rubinsztein, D.C. (2002). Mammalian, yeast, bacterial, and chemical chaperones

reduce aggregate formation and death in a cell model of oculopharyngeal muscular dystrophy. J. Biol. Chem. *277*, 12263-12269.

Carvalho, K.C., Cunha, I.W., Rocha, R.M., Ayala, F.R., Cajaiba, M.M., Begnami, M.D., Vilela, R.S., Paiva, G.R., Andrade, R.G., and Soares, F.A. (2011). GLUT1 expression in malignant tumors and its use as an immunodiagnostic marker. Clinics (Sao Paulo) *66*, 965-972.

Chen, X.H., Wu, W.G., and Ding, J. (2014). Aberrant TIG1 methylation associated with its decreased expression and clinicopathological significance in hepatocellular carcinoma. Tumour Biol. *35*, 967-971.

Cheng, H., Cenciarelli, C., Nelkin, G., Tsan, R., Fan, D., Cheng-Mayer, C., and Fidler, I.J. (2005). Molecular mechanism of hTid-1, the human homolog of Drosophila tumor suppressor l(2)Tid, in the regulation of NF-kappaB activity and suppression of tumor growth. Mol. Cell Biol. *25*, 44-59.

Ciocca, D.R., and Calderwood, S.K. (2005). Heat shock proteins in cancer: diagnostic, prognostic, predictive, and treatment implications. Cell Stress Chaperones. *10*, 86-103.

Clagett-Dame, M., and DeLuca, H.F. (2002). The role of vitamin A in mammalian reproduction and embryonic development. Annu. Rev. Nutr. *22*, 347-381.

Degos, L., Dombret, H., Chomienne, C., Daniel, M.T., Miclea, J.M., Chastang, C., Castaigne, S., and Fenaux, P. (1995). All-trans-retinoic acid as a differentiating agent in the treatment of acute promyelocytic leukemia. Blood *85*, 2643-2653.

Demand, J., Luders, J., and Hohfeld, J. (1998). The carboxy-terminal domain of Hsc70 provides binding sites for a distinct set of chaperone cofactors. Mol. Cell Biol. *18*, 2023-2028.

Edwards, K.M., and Munger, K. (2004). Depletion of physiological levels of the human TID1 protein renders cancer cell lines resistant to apoptosis mediated by multiple exogenous stimuli. Oncogene *23*, 8419-8431.

Guo, F., Sigua, C., Bali, P., George, P., Fiskus, W., Scuto, A., Annavarapu, S., Mouttaki, A., Sondarva, G., Wei, S., et al. (2005). Mechanistic role of heat shock protein 70 in Bcr-Abl-mediated resistance to apoptosis in human acute leukemia cells. Blood *105*, 1246-1255.

Hamelin, C., Cornut, E., Poirier, F., Pons, S., Beaulieu, C., Charrier, J.P., Haidous, H., Cotte, E., Lambert, C., Piard, F., et al. (2011). Identification and verification of heat shock protein 60 as a potential serum marker for colorectal cancer. FEBS J. *278*, 4845-4859.

Hamrita, B., Chahed, K., Kabbage, M., Guillier, C.L., Trimeche, M., Chaieb, A., and Chouchane, L. (2008). Identification of tumor antigens that elicit a humoral immune response in breast cancer patients' sera by serological proteome analysis (SERPA). Clin. Chim. Acta *393*, 95-102.

Huang, L., Yu, Z., Zhang, T., Zhao, X., and Huang, G. (2014). HSP40 interacts with pyruvate kinase M2 and regulates glycolysis and cell proliferation in tumor cells. PLoS One *9*, e92949.

Hwang, Y.J., Lee, S.P., Kim, S.Y., Choi, Y.H., Kim, M.J., Lee, C.H., Lee, J.Y., and Kim, D.Y. (2009). Expression of heat shock protein 60 kDa is upregulated in cervical cancer. Yonsei Med. J. *50*, 399-406.

Ito, N., Kamiguchi, K., Nakanishi, K., Sokolovskya, A., Hirohashi, Y., Tamura, Y., Murai, A., Yamamoto, E., Kanaseki, T., Tsukahara, T., et al. (2016). A novel nuclear DnaJ protein, DNAJC8, can suppress the formation of spinocerebellar ataxia 3 polyglutamine aggregation in a J-domain independent manner. Biochem. Biophys. Res. Commun. *474*, 626-633.

Jing, C., El-Ghany, M.A., Beesley, C., Foster, C.S., Rudland, P.S., Smith, P., and Ke, Y. (2002). Tazarotene-induced gene 1 (TIG1) expression in prostate carcinomas and its relationship to tumorigenicity. J. Natl. Cancer Inst. *94*, 482-490.

Kim, S.W., Chao, T.H., Xiang, R., Lo, J.F., Campbell, M.J., Fearns, C., and Lee, J.D. (2004). Tid1, the human homologue of a Drosophila tumor suppressor, reduces the malignant activity of ErbB-2 in carcinoma cells. Cancer Res. *64*, 7732-7739.

Kim, S.W., Hayashi, M., Lo, J.F., Fearns, C., Xiang, R., Lazennec, G., Yang, Y., and Lee, J.D. (2005). Tid1 negatively regulates the migratory potential of cancer cells by inhibiting the production of interleukin-8. Cancer Res. *65*, 8784-8791.

Kwok, W.K., Pang, J.C., Lo, K.W., and Ng, H.K. (2009). Role of the RARRES1 gene in nasopharyngeal carcinoma. Cancer Genet. Cytogenet. *194*, 58-64.

Lee, Y.M., Lee, J.O., Jung, J.H., Kim, J.H., Park, S.H., Park, J.M., Kim, E.K., Suh, P.G., and Kim, H.S. (2008). Retinoic acid leads to cytoskeletal rearrangement through AMPK-Rac1 and stimulates glucose uptake through AMPK-p38 MAPK in skeletal muscle cells. J. Biol. Chem. *283*, 33969-33974.

Li, C., Zhang, G., Zhao, L., Ma, Z., and Chen, H. (2016). Metabolic reprogramming in cancer cells: glycolysis, glutaminolysis, and Bcl-2 proteins as novel therapeutic targets for cancer. World J. Surg. Oncol. *14*, 15.

Maehara, Y., Oki, E., Abe, T., Tokunaga, E., Shibahara, K., Kakeji, Y., and Sugimachi, K. (2000). Overexpression of the heat shock protein HSP70 family and p53 protein and prognosis for patients with gastric cancer. Oncology *58*, 144-151.

Medina, R.A., and Owen, G.I. (2002). Glucose transporters: expression, regulation and cancer. Biol Res. *35*, 9-26.

Mitra, A., Shevde, L.A., and Samant, R.S. (2009). Multi-faceted role of HSP40 in cancer. Clin. Exp. Metastasis. *26*, 559-567.

Miyake, H., Muramaki, M., Kurahashi, T., Yamanaka, K., Hara, I., and Fujisawa, M. (2006). Enhanced expression of heat shock protein 27 following neoadjuvant hormonal therapy is associated with poor clinical outcome in patients undergoing radical prostatectomy for prostate cancer. Anticancer Res. *26*, 1583-1587.

Mizuiri, H., Yoshida, K., Toge, T., Oue, N., Aung, P.P., Noguchi, T., and Yasui, W. (2005). DNA methylation of genes linked to retinoid signaling in squamous cell carcinoma of the esophagus: DNA methylation of CRBP1 and TIG1 is associated with tumor stage. Cancer Sci. *96*, 571-577.

Mueckler, M., and Thorens, B. (2013). The SLC2 (GLUT) family of membrane transporters. Mol. Aspects Med. *34*, 121-138.

Murphy, M.E. (2013). The HSP70 family and cancer. Carcinogenesis. *34*, 1181-1188.

Nagpal, S., Patel, S., Asano, A.T., Johnson, A.T., Duvic, M., and Chandraratna, R.A. (1996). Tazarotene-induced gene 1 (TIG1), a novel retinoic acid receptor-responsive gene in skin. J. Invest. Dermatol. *106*, 269-274.

Oka, M., Sato, S., Soda, H., Fukuda, M., Kawabata, S., Nakatomi, K., Shiozawa, K., Nakamura, Y., Ohtsuka, K., and Kohno, S. (2001). Autoantibody to heat shock protein Hsp40 in sera of lung cancer patients. Jpn. J. Cancer Res. *92*, 316-320.

Peng, Z., Shen, R., Li, Y.W., Teng, K.Y., Shapiro, C.L., and Lin, H.J. (2012). Epigenetic repression of RARRES1 is mediated by methylation of a proximal promoter and a loss of CTCF binding. PLoS One *7*, e36891.

Qiu, X.B., Shao, Y.M., Miao, S., and Wang, L. (2006). The diversity of the DnaJ/Hsp40 family, the crucial partners for Hsp70 chaperones. Cell Mol. Life Sci. *63*, 2560-2570.

Salani, B., Ravera, S., Amaro, A., Salis, A., Passalacqua, M., Millo, E., Damonte, G., Marini, C., Pfeffer, U., Sambuceti, G., et al. (2015). IGF1 regulates PKM2 function through Akt phosphorylation. Cell

Cycle *14*, 1559-1567.

Shutoh, M., Oue, N., Aung, P.P., Noguchi, T., Kuraoka, K., Nakayama, H., Kawahara, K., and Yasui, W. (2005). DNA methylation of genes linked with retinoid signaling in gastric carcinoma: expression of the retinoid acid receptor beta, cellular retinol-binding protein 1, and tazarotene-induced gene 1 genes is associated with DNA methylation. Cancer *104*, 1609-1619.

Shyu, R.Y., Wang, C.H., Wu, C.C., Chen, M.L., Lee, M.C., Wang, L.K., Jiang, S.Y., and Tsai, F.M. (2016). Tazarotene-induced gene 1 enhanced cervical cell autophagy through transmembrane protein 192. Mol. Cells *39*, 877-887.

Siddikuzzaman, Guruvayoorappan, C., and Berlin Grace, V.M. (2011). All trans retinoic acid and cancer. Immunopharmacol. Immunotoxicol. *33*, 241-249.

Sterrenberg, J.N., Blatch, G.L., and Edkins, A.L. (2011). Human DNAJ in cancer and stem cells. Cancer Lett. *312*, 129-142.

Syken, J., De-Medina, T., and Munger, K. (1999). TID1, a human homolog of the Drosophila tumor suppressor l(2)tid, encodes two mitochondrial modulators of apoptosis with opposing functions. Proc. Natl. Acad. Sci. USA 96, 8499-8504.

Takai, N., Kawamata, N., Walsh, C.S., Gery, S., Desmond, J.C., Whittaker, S., Said, J.W., Popoviciu, L.M., Jones, P.A., Miyakawa, I., et al. (2005). Discovery of epigenetically masked tumor suppressor genes in endometrial cancer. Mol. Cancer Res. *3*, 261-269.

Tsai, F.M., Wu, C.C., Shyu, R.Y., Wang, C.H., and Jiang, S.Y. (2011). Tazarotene-induced gene 1 inhibits prostaglandin E2-stimulated HCT116 colon cancer cell growth. J. Biomed. Sci. *18*, 88.

Wang, X., Saso, H., Iwamoto, T., Xia, W., Gong, Y., Pusztai, L., Woodward, W.A., Reuben, J.M., Warner, S.L., Bearss, D.J., et al. (2013). TIG1 promotes the development and progression of inflammatory breast cancer through activation of Axl kinase. Cancer Res. *73*, 6516-6525.

Warburg, O., Wind, F., and Negelein, E. (1927). The metabolism of tumors in the body. J Gen. Physiol. *8*, 519-530.

Whitley, D., Goldberg, S.P., and Jordan, W.D. (1999). Heat shock proteins: a review of the molecular chaperones. J. Vasc. Surg. *29*, 748-751.

Wu, C.C., Shyu, R.Y., Chou, J.M., Jao, S.W., Chao, P.C., Kang, J.C., Wu, S.T., Huang, S.L., and Jiang, S.Y. (2006). RARRES1 expression is significantly related to tumour differentiation and staging in colorectal adenocarcinoma. Eur. J. Cancer *42*, 557-565.

Wu, C.C., Tsai, F.M., Shyu, R.Y., Tsai, Y.M., Wang, C.H., and Jiang, S.Y. (2011). G protein-coupled receptor kinase 5 mediates Tazarotene-induced gene 1-induced growth suppression of human colon cancer cells. BMC Cancer *11*, 175.

Yan, Y., Li, Z., Xu, X., Chen, C., Wei, W., Fan, M., Chen, X., Li, J.J., Wang, Y., and Huang, J. (2016). All-trans retinoic acids induce differentiation and sensitize a radioresistant breast cancer cells to chemotherapy. BMC Complement Altern. Med. *16*, 113.

Yanatatsaneejit, P., Chalermchai, T., Kerekhanjanarong, V., Shotelersuk, K., Supiyaphun, P., Mutirangura, A., and Sriuranpong, V. (2008). Promoter hypermethylation of CCNA1, RARRES1, and HRASLS3 in nasopharyngeal carcinoma. Oral Oncol. *44*, 400-406.

Yang, W., and Lu, Z. (2013). Regulation and function of pyruvate kinase M2 in cancer. Cancer Lett. *339*, 153-158.

Yang, W., Zheng, Y., Xia, Y., Ji, H., Chen, X., Guo, F., Lyssiotis, C.A., Aldape, K., Cantley, L.C., and Lu, Z. (2012). ERK1/2-dependent phosphorylation and nuclear translocation of PKM2 promotes the Warburg effect. Nat. Cell Biol. *14*, 1295-1304.

Yoshidomi, K., Murakami, A., Yakabe, K., Sueoka, K., Nawata, S., and Sugino, N. (2014). Heat shock protein 70 is involved in malignant behaviors and chemosensitivities to cisplatin in cervical squamous cell carcinoma cells. J. Obstet. Gynaecol. Res. *40*, 1188-1196.

Yu, M., Yongzhi, H., Chen, S., Luo, X., Lin, Y., Zhou, Y., Jin, H., Hou, B., Deng, Y., Tu, L., et al. (2017). The prognostic value of GLUT1 in cancers: a systematic review and meta-analysis. Oncotarget *8*, 43356-43367.

Zhang, J., Liu, L., and Pfeifer, G.P. (2004). Methylation of the retinoid response gene TIG1 in prostate cancer correlates with methylation of the retinoic acid receptor beta gene. Oncogene *23*, 2241-2249.